

Simple Microwave Synthesis of CdO/Clay Nanocomposites and Investigation its Application for Degradation of MB

Mohammad Mehdi Foroughi¹ · Abbas Pardakhty² · Mehdi Ranjbar³

Received: 13 December 2016 / Published online: 10 February 2017
© Springer Science+Business Media New York 2017

Abstract In this study, we applied a novel synthesis route for producing CdO–Clay nanocomposite by simple microwave method with the aid of bentonite clay. The effects of difference microwave powers on the morphology and particle size of final products were investigated. Besides, degradation of methylene blue (MB) dye in water was applied to examine the photocatalytic application of CdO–Clay nanocomposite under visible light irradiation. Scanning electron microscopy (SEM) results reveal that microwave power has undeniable impact on the morphology and particle size of final nanocomposite. Photoluminescence spectra show a blue shift when the nanoparticles are prepared in the presence of the clay minerals. The as-synthesized products were characterized by X-ray diffraction, SEM, transmission electron microscopy, and photoluminescence spectroscopy. This Clay nanocomposite act as efficient photocatalysts showing higher yield in the photocatalytic decomposition of MB dye in water than the corresponding CdO powder without clay prepared under similar experimental conditions.

Keywords CdO–Clay · Nanocomposite · Microwave method · Photocatalysis

Introduction

Semiconductor-assisted photocatalysis method has been studied widely for the removal of dyes and toxic organic compounds from wastewater as the low cost, large-scale, cleaner, and greener technology [1–3]. Clay minerals and clay-derived

✉ Mehdi Ranjbar
Mehdi.Ranjbar@outlook.com

¹ Department of Chemistry, Kerman Branch, Islamic Azad University, Kerman, Iran

² Pharmaceutics Research Center, Institute of Neuropharmacology, Kerman University of Medical Sciences, Kerman, Iran

³ Young Researchers and Elite Club, Kerman Branch, Islamic Azad University, Kerman, Iran

materials offer universal and commercial opportunities for many diverse applications including those based on their unique surface properties. Clays are widely used as the development of nanostructures materials because this materials are inexpensive, non-hazardous, easily available, flexible, and very promising supports for the design and preparation of biocompatible electrocatalyst material. A large number of ion exchange sites available in clays are also beneficial for incorporation of electroactive species and nanoparticles. Cadmium oxide (CdO) which occurs naturally in the rare mineral brown or red monteponite single crystals, is an n-type oxide belonging to the II–VI group. Its direct and indirect band gaps are in the range of 2.2–2.5 and 1.36–1.98 eV respectively [4–7]. Such a difference in both direct and indirect band gaps is attributed to intrinsic Cadmium and Oxygen vacancies. Due to its ionic nature coupled with its low electrical resistivity and high optical transmission in the visible region, nano-scaled CdO are suitable candidate for several technological applications in various fields such as solar cells [8, 9], phototransistors [10], photodiodes [11], transparent electrodes and gas sensors [12]. Numerous synthetic physical and chemical processes, including hydrothermal, template assisted, solvothermal, mechanochemical, thermal decomposition, photosynthetic and sonochemical methodologies have been employed to prepare CdO nanostructures [13–17]. In the current era, application of microwave energy to heat chemical reactions has attracted a considerable amount of attention due to its many successful applications in the material sciences, nanotechnology and biochemical processes [18–21]. By comparing the microwave method and the conventional heating methods, it was clearly found that the microwave route have many advantages involving rapid and homogeneous volumetric heating, high reaction rate, short reaction time, and enhanced reaction selectivity. The objective of this work is to investigate synthesis and characterization of CdO–Clay nanocomposites through the fast and convenient microwave method. In addition, morphology and particles size of final products were investigated in difference microwave power. To examine the ability of CdO–Clay nanocomposites as the semiconductor photocatalyst decolorization of methylene blue under visible light irradiation was done.

Experimental

Materials and physical measurements

All the chemical reagents used in our experiments were of analytical grade and were used as received without further purification. XRD patterns were recorded by a Rigaku D-max C III, X-ray diffractometer using Ni-filtered Cu K α radiation of Kashan-Iran University. Microscopic morphology of products was visualized by SEM (LEO 1455VP) and Transmission electron microscopy (TEM) images were obtained on a Philips EM208 transmission electron microscope with an accelerating voltage of 200 kV in Shahid Bahonar University Kerman-IRAN. UV–Vis diffuse reflectance spectroscopy analysis was carried out using Shimadzu UV-2600 UV–Vis spectrophotometer with an integrating sphere attachment and BaSO₄ was used as reference.

Synthesis of CdO Nanostructures

The CdO was prepared by a solid-state thermal decomposition with the aid of $\text{Cd}(\text{OAc})_2 \cdot 2\text{H}_2\text{O}$ without any surfactants or additive. In the typical procedure, 1 g of $\text{Cd}(\text{OAc})_2 \cdot 2\text{H}_2\text{O}$ powder was put into a small quartz boat. The quartz boat was entered into the proper position of the tube furnace and it was held in the heating zone at 250 °C for 2 h and then it was slowly dragged out of the furnace. The sample was naturally cooled down in ambient conditions.

Synthesis of CdO–Clay Nanocomposites

0.5 g of the as-obtained CdO was dissolved in 20 mL of deionized water. Then, 2 g of the clay mineral was dispersed in 10 mL deionized water and added to the above mentioned solution under stirring at 80 °C. Afterwards, the mixture was loaded into a microwave Teflon container, and the reaction was performed in a microwave digestion system under various conditions (Table 1).

Photocatalysis Experiments

In order to evaluate the photocatalytic activity of the CdO–Clay nanocomposites, degradation of methylene blue dye under visible light irradiation was performed. In a typical photocatalysis experiment CdO–Clay nanocomposites (30 mg) were added into a glass beaker containing 150 mL of aqueous dye solution (5 mg/L), and then dispersed by stirring for 30 min at 25 °C in darkness to establish adsorption–desorption equilibrium between the dye molecules and CdO–Clay nanocomposites surface. Later, a series of UV lamps (6×15 W, Philips) were switched on a 30 cm distance over the suspension surface. Finally, the absorbance spectra of the methylene blue solution were recorded by a UV–Vis spectrophotometer (Shimadzu UV–Vis spectrometer) and the decolorization rate was calculated according to the absorbance change.

Results and Discussion

Crystalline structure and phase purity of as-prepared products have been determined using XRD ($10 < 2\theta < 80$) technique. Figure 1a–c shows the XRD patterns of clay, CdO obtained from solid-state thermal decomposition, $\text{Cd}(\text{OAc})_2$ was heated at

Table 1 Reaction conditions for CdO–Clay nanocomposites

Sample no	Power (W)	Time (min)	Degradation (%)
1	600	8	80
2	750	8	77
3	900	8	76
4	600	8	74
CdO	–	–	58

250 °C, and CdO–Clay nanocomposites (sample 3), synthesized by microwave method, respectively. All reflection peaks of Fig. 1b are well indexed to cubic (fcc) phase CdO (JCPDS No. 75-0594). A comparison between the XRD patterns for clay and the CdO–clay nanocomposite demonstrate that peaks related CdO in CdO–clay nanocomposite are shifted toward the higher wavelength indicating formation of nanocomposite. Effects of difference microwave powers on the morphology and particles size of CdO–clay nanocomposites were investigated through the SEM analysis. Figure 2a–d show the SEM images of sample 1–4 corresponding to the microwave powers 450, 600, 750, and 900 W, respectively. According to the Fig. 2a, CdO–clay nanocomposite, 450 W, mainly consist of sheet nanostructures. Increasing microwave power from 450 to 600 W causes the size of sheets to decrease, as shown in Fig. 2 b. Further increasing in microwave power from 600 to 750 W (Fig. 2c) and 900 W (Fig. 2d) causes to change the morphology from sheet structures to the rod nanostructure. To further investigate the details of morphology TEM image was taken from the sample 3, as shown in Fig. 3. Figure 3 shows the presence of CdO nanoparticles covering the clay where remain assembled possibly by bonding to the silanol groups at the external surface of the clay. Figure 4 shows emission (centered at 449 nm) and emission (centered at 510 nm) spectra corresponding to CdO–Clay nanocomposites (sample 3) and CdO nanoparticles, respectively. The emission spectrum shows a blue shift in CdO–Clay nanocomposites compared to that of the CdO nanoparticles. This blue shift means increasing band gap energy due to particle confinement effect in that immobilization of CdO produced in nanosize of CdO particle. Similar pattern of shift was also reported by other similar nanocomposite works [22, 23]. FTIR analysis of CdO–Clay nanocomposites (sample 3) was performed in the range of 400–4000 cm^{-1}

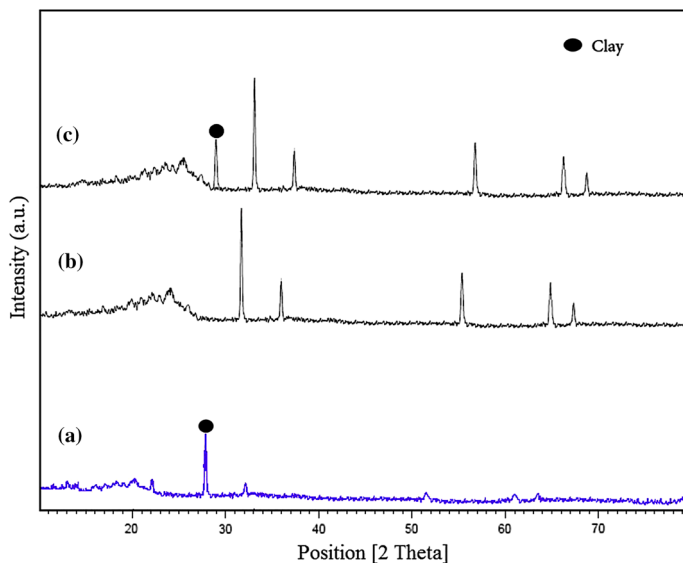


Fig. 1 XRD patterns of *a* clay *b* CdO nanoparticles prepared by thermal decomposition *c* CdO–Clay nanocomposites (sample 3)

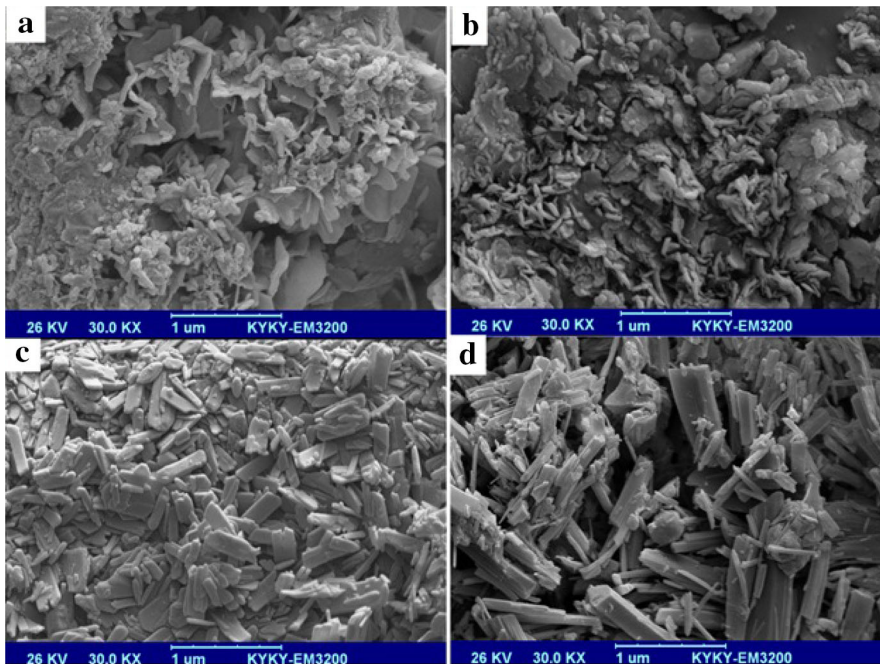


Fig. 2 SEM images of the CdO–Clay nanocomposites **a** 450 W **b** 600 W **c** 750 W **d** 900 W

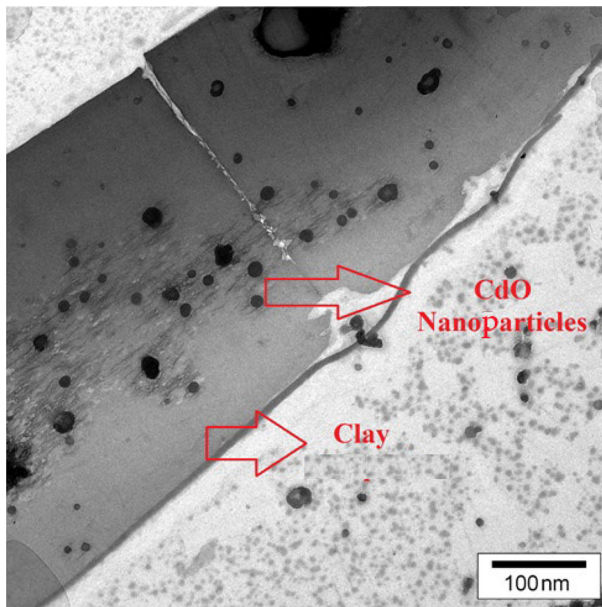


Fig. 3 TEM image of the CdO–Clay nanocomposites (sample 3)

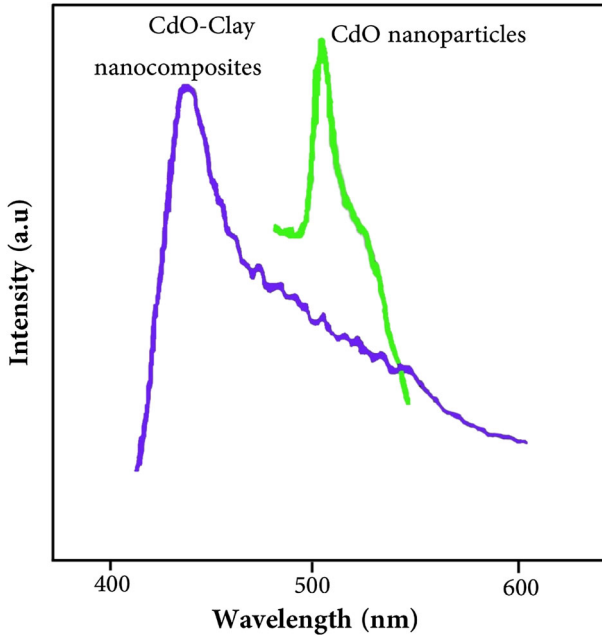


Fig. 4 Room temperature PL spectra of CdO nanoparticles and CdO–Clay nanocomposites (sample 3)

(Fig. 5). The broad absorption band centered at 3400 cm^{-1} and a weak peak at 1612 cm^{-1} are attributable to the $\nu(\text{OH})$ stretching and bending vibrations, respectively [24]. Besides, peaks at $1050\text{--}1150\text{ cm}^{-1}$ belong to Cd–O–Si and Cd–O–Al in clay-nanocomposites. The less intense peaks located at 542 and 780 cm^{-1} are all associated to the stretching Cd–O modes [25–28]. The presence of these four characteristic Cd–O stretching modes supports the phase purity of the CdO nanoparticles. To evaluate the decomposition of methylene blue (MB), as-

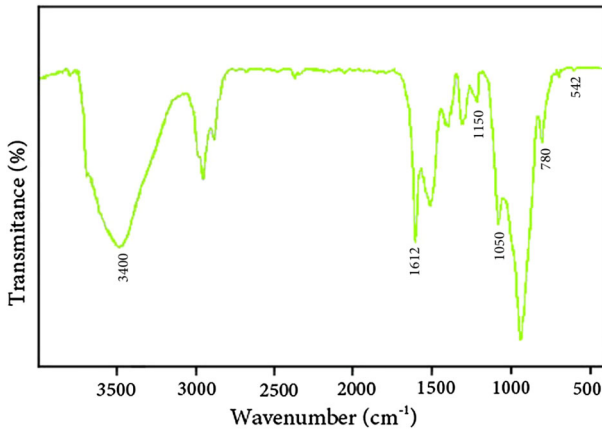


Fig. 5 FT-IR spectrum of CdO–Clay nanocomposites (sample 3)

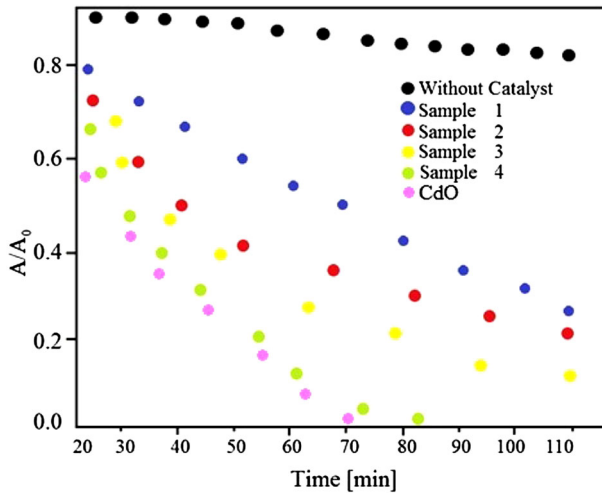


Fig. 6 Photodecolorization of methylene blue (MB) under UV illumination by blank, CdO nanoparticles, and CdO–Clay nanocomposites (samples 1–4)

synthesized CdO–Clay nanocomposites were used as photocatalyst. Figure 6 exhibits the plot of the remaining dye concentration (A/A_0) versus time intervals for the photocatalytic reaction of CdO–Clay nanocomposites. The dye degradation rate on the surface of CdO–Clay nanocomposites is calculated by the following:

$$\text{Degradation rate (\%)} = (A_0 - A)/A_0 \times 100$$

where A_0 and A are initial concentration and changed absorbencies of dye after ultraviolet irradiation, respectively. Degradation rates of CdO–Clay nanocomposites (samples 1–4) and CdO nanoparticles are shown in Fig. 6. It can be seen that in the absence of CdO–Clay nanocomposites, an almost negligible amount of methylene blue (MB) degradation is observable while the maximum degradation rate is 80% in the presence of CdO–Clay nanocomposites (samples 1) after 110 min. The significant improvement of MB degradation by CdO–clay nanocomposite was related to the higher dispersion of CdO nanoparticles on the surface of clay which causes interaction of CdO with MB dye to increase. In comparison to other works, based on the author's knowledge, it is the first report on the synthesis of CdO–clay nanocomposite through the simple, low cost, and scale-up route. Besides, in the presence of clay, CdO nanoparticles have higher band gap in comparison with CdO nanoparticles which causes the amount of degradation of organic dye to increase and make it more suitable for industrial waste water applications [29–32].

Conclusion

In this manuscript, the CdO–Clay nanocomposite was successfully synthesized with the aid of CdO nanoparticles, synthesized through the simple thermal decomposition method, and bentonite clay through the rapid and facile microwave method. Four

microwave powers, 450, 600, 700, and 900 W were applied to investigate their effect on the morphology and particle size of CdO–Clay nanocomposite. In this research, MB dye solution has been used as the inorganic pollutant, showing better efficiency the CdO–clay samples than CdO NP.

Acknowledgements Authors are grateful to council of Azad University of Kerman, Institute of Neuropharmacology, Kerman University of Medical Sciences, Shimi Gostar-E-Botya Samangan Company, and Padideh Noavaran Nano Bonyan Company, Iran.

References

1. P. Rajaei and M. Ranjbar (2016). *J. Mater. Sci. Mater. Electron.* **27**, 1708.
2. M. Ramezani, A. Davoodi, A. Malekizad, and S. M. Hosseinpour-Mashkani (2015). *J. Mater. Sci. Mater. Electron.* **26**, (6), 3957.
3. A. Sobhani-Nasab, M. Maddahfar, and S. M. Hosseinpour-Mashkani (2016). *J. Mol. Liq.* **216**, 1.
4. S. Akın, G. Karanfil, A. Gültekin, and S. Sonmezoglu (2013). *J. Alloys Compd.* **579**, 272.
5. K. Kaviyarasu, E. Manikandan, P. Paulraj, S. B. Mohamed, and J. Kennedy (2014). *J. Alloys Compd.* **593**, 67.
6. A. Tadjarodi, M. Imani, and H. Kerdari (2013). *Int. Nano Lett.* **3**, 43.
7. S. Aldwayyan, F. M. Al-Jekhedab, M. Al-Noaimi, B. Hammouti, T. B. Hadda, M. Suleiman, and I. Warad (2013). *Int. J. Electrochem. Sci.* **8**, 10506.
8. C. Sravani, K. T. R. Reddy, O. M. Hussain, and P. J. Reddy (1996). *J. Solar Energy Soc. India* **1**, 6.
9. L. M. Su, N. Grote, and F. Schmitt (1984). *Electron. Lett.* **20**, 716.
10. R. Kondo, H. Okimura, and Y. Sakai (1971). *Jpn. J. Appl. Phys.* **10**, 1547.
11. F. A. Benko and F. P. Koffyberg (1986). *Solid State Commun.* **57**, 901.
12. Shiori A Jpn. Patent No. 7 (1997) 909.
13. N. M. Al-Hada, E. B. Saion, A. H. Shaari, M. A. Kamarudin, M. Flaifel, S. Ahmad, and A. Gene (2014). *Mater. Sci. Semicond. Process.* **26**, 460.
14. A. Askarinejad and A. Morsali (2009). *Chem. Eng. J.* **150**, 569.
15. G. R. Khayati, H. Dalvand, E. Darezereshki, and A. Irannejad (2014). *Mater. Lett.* **115**, 272.
16. A. M. El Sayed and A. Ibrahim (2014). *Mater. Sci. Semicond. Process.* **26**, 320.
17. A. M. Bazargan, S. M. A. Fateminia, M. Esmaeilpour Ganji, and M. A. Bahrevar (2009). *Chem. Eng. J.* **155**, 523.
18. A. Mohadesi, M. Ranjbar, and A. Salmanipour (2016). *J. Mater. Sci. Mater. Electron.* **27**, 9073.
19. P. Junploy, S. Thongtem, and T. Thongtem (2013). *Superlattices Microstruct.* **57**, 1.
20. M. M. Foroughi and M. Ranjbar (2017). *J. Mater. Sci. Mater. Electron.* **28**, 1359.
21. K. Mohammadi, M. Ranjbar, and H. Targholizadeh (2016). *J. Mater. Sci. Mater. Electron.* **27**, 7829.
22. Y. Zhi, Y. Li, Q. Zhang, and H. Wang (2010). *Langmuir* **26**, (19), 15546.
23. M. Akkari, P. Aranda, H. Ben Rhaïem, A. B. Haj-Amara, and E. Ruiz-Hitzky (2016). *Appl. Clay Sci.* **131**, 131.
24. S. M. Hosseinpour-Mashkani and M. Ramezani (2014). *Mater. Lett.* **130**, 259.
25. K. Gurumurugan, D. Mangalaraj, and S. K. Narayandass (1996). *J. Electron. Mater.* **25c**, 765.
26. T. Kuo and M. H. Huang (2006). *J. Phys. Chem. B.* **110**, 13717.
27. M. Benhaliliba, C. E. Benouis, and A. S. Tiburcio (2012). *J. Lumin.* **132**, 2653.
28. M. A. Flores, P. R. Castanedo, D. G. Torres, S. A. Toms, A. J. G. Mendoza, and A. O. Zelaya (2010). *J. Lumin.* **130**, 2500.
29. V. Veeraputhiran, V. Gomathinayagam, A. Udhaya, K. Franci, and K. Kathrunnisa (2015). *J. Adv. Chem. Sci.* **1**, 17.
30. F. T. Thema, P. Beukes, A. Gurib-Fakima, and M. Maazaa (2015). *J. Alloys Compd.* **646**, 1043.
31. D. D. Vijaykarthik, M. Kirithika, N. Prithivikumar, and N. Jeyakumar (2014). *IJND* **5**, 557.
32. P. A. Radi, A. G. Brito-Madurro, J. M. Madurro, and N. O. Dantas (2006). *Braz. J. Phys.* **36**, 2.